Characterization of the Dexniguldipine Binding Site in the Multidrug Resistance-Related Transport Protein P-Glycoprotein by Photoaffinity Labeling and Mass Spectrometry

CHRISTOPH BORCHERS,[1] RAINER BOER, KURT KLEMM, VOLKER FIGALA, THOMAS DENZINGER, WOLF-RÜDIGER ULRICH, SABINE HAAS, WOLFGANG ISE, VOLKER GEKELER, and MICHAEL PRZYBYLSKI

Department of Chemistry, Analytical Chemistry, University of Konstanz, Konstanz, Germany (C.B., T.D., M.P.); and Byk Gulden Lomberg GmbH, Konstanz, Germany (R.B., K.K., V.F., W.-R.U., S.H., W.I., V.G.)

This article is available online at http://molpharm.aspetjournals.org

ABSTRACT

Human P-glycoprotein (P-gp), an integral membrane transport protein, is responsible for the efflux of various drugs, including cytostatics from cancer cells leading to multidrug resistance. P-gp is composed of two homologous half domains, each carrying one nucleotide binding site. The drug extrusion is ATP-dependent and can be inhibited by chemosensitizers, such as the dihydropyridine derivative dexniguldipine-HCl, through direct interaction with P-gp. To evaluate the mechanism(s) of chemosensitization and identify the binding sites of dexniguldipine-HCl, a tritium-labeled azido analog of dexniguldipine, [³H]B9209-005, was used as a photoaffinity probe. Using the multidrug resistant T-lymphoblastoid cell line CCRF-ADR5000, two proteins were specifically labeled in membranes by [³H]B9209-005. These proteins were identified by immunoprecipitation such as P-gp and its N-terminal fragment. The membranes were solubilized and the labeled P-gp proteins first isolated by lectin-chromatography and then digested with trypsin. SDS-polyacrylamide gel electrophoresisanalysis of the digest revealed a major radioactive 7-kDa fragment. The tryptic fragments were separated by high-performance liquid chromatography and analyzed by matrix-assisted laser desorption/ionization mass spectrometry (MALDI-MS). The MS results, corroborated by MALDI-MS of peptides after one step of Edman analysis, identified the radioactive 7-kDa band as the dexniguldipine-bound, tryptic P-gp peptide, 468–527. This sequence region is flanked by the Walker motifs A and B of the N-terminal ATP-binding cassette suggesting direct interaction of the chemosensitizer with the nucleotide binding site is involved in the mechanism of chemosensitization.

Tumor cells in vitro and in vivo can develop simultaneous resistance to the lethal effects of a variety of cytotoxic drugs (Endicott and Ling, 1989). This so-called multidrug resistance (MDR) is a major limiting factor for the efficacy of cancer chemotherapy. Currently, a variety of mechanisms are known that can lead to drug resistance, including reduced cellular drug accumulation, increased detoxification, intracellular vesicularization of drugs, altered enzymatic activities, up- or down-regulation of targets, and enhanced DNA repair (Hayes and Wolf, 1990). One important resistance mechanism is the transport out of cancer cells of chemically-unrelated cytotoxic drugs (such as anthracylines, *Vinca* alkaloids, colchicine, and taxanes) by the integral membrane phosphoglycoprotein P-glycoprotein (P-gp) under ATP hydrolysis, resulting in low and ineffective intracellular drug concentrations (Gottesman and Pastan, 1993). Although considerable progress has been made during the last few years, the mechanism of recognition and transport of such a broad spectrum of compounds is still poorly understood.

Reversal of multidrug resistance is of major clinical interest, and MDR-reversing agents called chemosensitizers have been intensively investigated (Raderer and Scheithauer, 1993; Sikic, 1993). The capability of reversing multidrug resistance in vitro by inhibiting the transport function of P-gp has been demonstrated for a number of compounds. One

ABBREVIATIONS: MDR, multidrug resistance; P-gp, P-glycoprotein; SDZ PSC 833, [3-keto-Bmt1]-[Val2]-cyclosporin; NBD, nucleotide-binding domain; [³H]B9209-005, 3-[3-(4-[³H]phenyl-4-phenyl-1-piperidinyl)propyl]-5-methyl-4(*R*)-(3-azidophenyl)-1,4-dihydro-2,6-dimethyl-pyridine-3,5-dicarboxylate; CHAPS, 3-[(3-cholamidopropyl)dimethylammonio]propanesulfonate; deoxy-BIGCHAP, *N,N*-bis-(3-D-gluconamidopropyl)deoxycholamide; PAGE, polyacrylamide gel electrophoresis; TBS, Tris-buffered saline; TBS/T, Tris-buffered saline containing 0.05% Tween 20; PITC, phenyl isothiocyanate; TFA, trifluoroacetic acid; HPLC, high-performance liquid chromatography; MALDI, matrix-assisted laser desorption/ionization; aa, amino acids.

of the best characterized agents is verapamil, whose first clinical trial was reported in 1984 (Present et al., 1984). Other compounds with MDR-reversing activity are cyclosporin A (Raderer and Scheithauer, 1993), SDZ PSC 833 (Fisher et al., 1994), and the 1,4-dihydropyridine derivative dexniguldipine-HCl (Reiter et al., 1994).

Human P-gp has an apparent molecular mass of 170 kDa and consists of 1280 amino acids encompassing two homologous halves (Chen et al., 1986). A short linker region connects the two domains and each half contains a nucleotide-binding domain (NBD) with "homology A" and "homology B" sequences commonly found in ATPases. Both ATP binding sites are catalytically active and are essential for drug extrusion (Azzaria et al., 1989; Urbatsch et al., 1995). A structural model of P-gp, derived from hydropathy plots, has been suggested to comprise six transmembrane-spanning α-helical segments, followed by a cytoplasmic NBD for each half of the molecule (Gottesman and Pastan, 1988; Juranka et al., 1989). A recent model has proposed two membrane-embedded sixteen-strand β-barrels, connected by short loops to two six-helix bundles beneath each barrel (Jones and George, 1998) (Fig. 7). A first insight into the three-dimensional architecture of P-gp was recently obtained by electron microscopy (Rosenberg et al., 1997) and structure determination at 2.5-nm low resolution, which, however, did not provide sufficient information for the understanding of the molecular transport mechanism.

Because drug binding must precede transport, the determination of the structural area involved in the binding is essential for elucidation of a structure-function relationship. Furthermore, the localization of the chemosensitization binding site can provide information on how this site is interacting with the drug binding and how the NBD is linked to drug transport and inhibition. To determine the binding area, domain mapping studies using photoaffinity analogs of drugs or chemosensitizers have been used in combination with immunoprecipitation (Safa, 1998). Detailed studies have been performed with a photoactive 1,4-dihydropyridine derivative, [3H]azidopine, and with [125I]iodoarylazidoprazosin (Greenberger, 1998) and have located two major regions of photoaffinity labeling, one within each half of the protein (Bruggemann et al., 1989; Greenberger et al., 1991; Morris et al., 1994).

In this study, we used a tritiated photoaffinity derivative of the chemosensitizer dexniguldipine-HCl ([3H]B9209-005) to probe the dihydropyridine binding site in P-gp. To obtain the photoreactive dexniguldipine derivative, an azido group replaced the nitro group in position 3 of the phenyl ring in the 4-phenyldihydropyridine moiety. As demonstrated earlier, this structural modification does not affect the chemosensitising potency of the molecule (Borchers et al., 1995; Boer et al., 1996). Although the two dihydropyridine derivatives, B9209-005 and azidopine, are related molecules, the photoreactive groups are in different positions, with azidopine carrying the azido group in the side chain of the dihydropyridine moiety. Compared with azidopine, B9209-005 has been shown to be a ~10-fold more potent chemosensitizer (Borchers et al., 1995) and, hence, seemed to be a suitable ligand for the elucidation of the chemosensitizer binding sites.

It has been shown previously, that [3H]B9209-005 is specifically photoincorporated into P-gp and its N-terminal fragment (Borchers et al., 1995; Boer et al., 1996). To identify the

binding site of dexniguldipine-HCl, we used a mass spectrometric approach instead of conventional immunoprecipitation with sequence-specific antibodies. In contrast to immunoprecipitation, mass spectrometry is, in general, not sequence-dependent, and even hydrophobic peptides, such as transmembrane domains, can be identified.

In the present study, we have used the combination of photoaffinity labeling and mass spectrometric peptide mapping (Przybylski et al., 1998) to localize the binding site of dexniguldipine-HCl. The results obtained are compared with those from azidopine and other photolabels and the location of the dihydropyridine binding site is discussed with respect to the two topological models of P-gp.

Experimental Procedures

Materials

Chemicals, Proteins, and Supplies. Dexniguldipine-HCl and [3H]B9209-005 were synthesized as described previously (Boer et al., 1996; Borchers et al., 1996). A specific radioactivity of 414 GBq/mmol (11.3 Ci/mmol) for [3H]B9209-005 was obtained. [3H]Azidopine was obtained from Amersham Biosciences (Braunschweig, Germany). The detergents CHAPS, deoxy-BIGCHAP, *n*-octylglucoside, deoxycholate, and Triton X-100 were purchased from Roche Applied Science (Mannheim, Germany), *N*-lauroylsarcosine and Nonidet P-40 were from Fluka (Buchs, Switzerland) and Zwittergent 3-12 was from Calbiochem (Bad Soden, Germany). Nitro blue tetrazolium and 5-bromo-4-chloro-3-indolyl phosphate were from Serva (Heidelberg, Germany). Tween 20, phenylisothiocyanate, and α-cyano-4-hydroxycinnamic acid were purchased from Aldrich (Deisendorf, Germany). Horse heart cytochrome C was from Fluka; bovine serum albumin, trypsin, and *Ricinus communis* agglutinin-120 (RCA-120) immobilized on agarose beads were obtained from Sigma (Deisendorf, Germany).

Cell Lines and Antibodies. The human T-lymphoblastoid cell line CCRF-CEM was obtained from the American Type Culture Collection (Manassas, VA). The selection of the multidrug-resistant CCRF-ADR5000 subcell line has been reported previously (Kimming et al., 1990). The cell lines were maintained as described previously (Borchers et al., 1995; Hofmann et al., 1995). The monoclonal antibody C219 was purchased from Centocor (Malvern, PA). Goat anti-mouse IgG and goat anti-rabbit IgG conjugated to alkaline phosphatase were purchased from Dianova (Hamburg, Germany). The production and purification of the polyclonal antibody 909 raised against a synthetic peptide corresponding to the P-gp amino acid sequence 909–927 was performed as described previously (Borchers et al., 1995).

Methods

Membrane Preparation and Photoaffinity Labeling. Plasma membrane preparation of CCRF-CEM and CCRF-ADR5000 cells and photoaffinity labeling with [3H]B9209-005 and [3H]azidopine have been reported in detail elsewhere (Borchers et al., 1995; Boer et al., 1996). Briefly, cells were homogenized in lysis buffer (10 mM NaCl, 1.5 mM MgCl$_2$, 10 mM Tris-HCl, pH 7.4) and membrane proteins were separated from cell nucleus and mitochondrial proteins by differential centrifugation. The resulting membrane pellet was resuspended in lysis buffer containing 50% glycerol. Protein concentration was determined by a bicinchoninic acid assay (Pierce, Rockford, Il) using bovine serum albumin as standard. For photoaffinity labeling, membranes (0.6 mg/ml) were incubated in PBS buffer, pH 7.4, in the presence of the photolabel for 1 h at 22°C in the dark. Irradiation was performed with a long-wave UV-lamp (Camag, Berlin, Germany) for 20 min at 4°C.

SDS-PAGE and Liquid Scintillation Counting. Gel electrophoretic analyses were performed according to the procedure of

Laemmli with a 8% polyacrylamide SDS-gel for separation of proteins and a 7.5 to 20% polyacrylamide gradient SDS-gel for separation of proteolytic fragments. The samples were diluted 1:1 in sample buffer (0.250 M Tris-HCl, 5% mercaptoethanol, 2% SDS, 0.01% bromphenol blue, 50% glycerol, pH 6.8) and applied to gels after incubation for 30 min at 22°C. Gels were stained with 0.25% Coomassie G250 in 25% isopropanol/10% acetic acid overnight and destained with 10% acetic acid. For radioactivity determination, gels were cut into 1-mm slices and incubated with Biolute-S (Zinsser, Frankfurt, Germany) for 3 h at 50°C. Radioactivity was quantified by liquid scintillation counting.

Solubilization and Detergent Exchange. To determine the P-gp solubilization efficiency by detergents, CCRF-ADR5000 membranes (0.6 $\mu g/\mu l$) were photolabeled with 1.6 μM [^{3}H]azidopine and homogenized with detergent solution (6% in 20 mM Tris-HCl, pH 7.4) at a final detergent concentration of 1% in a glass/glass homogenizer for 3 min at 4°C. After a 30-min incubation at 4°C, nonsolubilized proteins were removed by centrifugation (45,000 rpm; Optima TLX ultracentrifuge, rotor TLA-100.4, Beckmann, Karlsruhe, Germany) at 100,000g, 4°C. The supernatant was analyzed by SDS-PAGE. Solubilization with N-lauroylsarcosine was performed in the same manner. For purification of P-gp by RCA-120 chromatography, solubilization was carried out with 20 mM N-lauroylsarcosine in 20 mM Tris-HCl, pH 7.4.

Detergent exchange of P-gp solutions was performed by ultrafiltration using 500-μl Microcon centrifugal filter devices with a molecular mass cut-off of 100 kDa (Amicon, Eschborn, Germany). Ultrafiltration was carried out at 3000g and 22°C for 40 min with an Eppendorf centrifuge (Centrifuge 5415 C; Eppendorf, Germany) according to the manufacturer's instructions. After the first centrifugation, the Microcon centrifugal filter device was filled with 500 μl of detergent solution and centrifuged again for detergent exchange. This procedure was repeated four times.

Western Immunoblot Analysis. The membrane proteins were transferred onto Immobilon-P membranes (Millipore, Eschborn, Germany) using an electroblotting chamber (Hoefer Scientific Instruments, Inc., San Francisco, CA) in 25 mM Tris, 192 mM glycine, 1% SDS, and 20% (v/v) methanol, at 200 mA for 16 h. All of the following steps were performed at 22°C. After blocking with 5% nonfat dried milk in PBS for 2 h, the membrane was incubated with TBS (50 mM Tris-HCl, 0.15 M NaCl, pH 7.4) and diluted with P-gp–specific antibody, monoclonal antibody C219 (1 $\mu g/ml$), or polyclonal antibody 909 (1:500 dilution) for 2 h. After four washing steps (15 min each) with TBS containing 0.05% Tween 20 (TBS/T), the membrane was incubated for 2 h with anti-rabbit IgG and anti-mouse IgG, both alkaline-phosphatase–conjugated, in TBS/T at a dilution of 1:1000. After washing four times in TBS/T, the membrane was incubated for 10 to 15 min with 0.0016% 5-bromo-4-chloro-3-indolyl phosphate/0.0033% nitro blue tetrazolium in 100 mM Tris-HCl, 100 mM CaCl$_2$, 5 mM MgCl$_2$, pH 9. The reaction was quenched by addition of 0.02% EDTA in PBS buffer.

Enzymatic Digestion and Edman Coupling. Enzymatic digestion of [^{3}H]B9209-005–labeled, affinity-purified P-gp was performed with trypsin in 20 mM Tris-HCl, pH 7.7 in the presence of detergent (20 mM N-lauroylsarcosine, 1% CHAPS, and 1.4% n-octylglucoside, respectively). The digestion was carried out for 2.5 h at 37°C with a trypsin concentration of up to 100 $\mu g/ml$ corresponding to an enzyme to substrate ratio of approximately 20:1. The reaction was quenched by cooling the solution to -20°C.

Manual Edman coupling of [^{3}H]B9209-005–labeled P-gp peptides after trypsin digestion and HPLC separation was performed as described previously (Nielsen et al., 1990). The lyophilized peptides were redissolved in 50 μl of isopropanol and incubated at 30°C for 4 h with 100 μl of 5% phenyl isothiocyanate (PITC) in pyridine. The solvents and remaining PITC were removed by lyophilization.

Lectin Chromatography. Chromatography with RCA-120 immobilized on agarose beads was performed with the [^{3}H]B9209-005 photolabeled CCRF-ADR5000 membranes solubilized in 20 mM N-lauroylsarcosine, 20 mM Tris-HCl, pH 7.7 (solubilization buffer). All chromatographic steps were performed at 4°C. An Econo chromatography column (Bio-Rad, Freiburg, Germany) was filled with RCA$_{120}$ beads (gel matrix volume of up to 10 ml) and equilibrated with 10 gel volumes of solubilization buffer. The column was loaded with the solubilized membranes (5–25 ml) and incubated for 2 h under slow rotation (batch approach) or separated at a flow rate of 0.5–1 ml/min. After draining off supernatant (batch approach) or sample flow through the column, the column was washed with solubilization buffer (5 times the gel matrix volume). Elution was performed in 0.5-ml fractions by the addition of 0.2 M methyl β-D-galactopyranoside in solubilization buffer (elution volume = five times the gel matrix volume). Individual fractions of 0.5 to 1 ml were collected and analyzed by SDS-PAGE.

HPLC. Separation of proteolytic fragments of [^{3}H]B9209-005 photolabeled P-gp after lectin chromatography and detergent exchange was performed with a Bio-Rad HPLC solvent delivery system model 2700 equipped with a UV/VIS detector system model 1706 (Bio-Rad). Chromatography was carried out on a Vydac Protein C$_4$ (250 × 4.6 mm, 5-μm particle size) reversed-phase column (Macherey-Nagel, Duisburg, Germany) using a binary gradient of 0.1% aqueous TFA (A) and 0.1% TFA in acetonitrile/isopropanol [4/1 (v/v)] (B); 0 to 5 min, 5% B; 5 to 45 min, 5 to 90% B; 45 to 50 min, 90% B; 50 to 55 min, 90–5% B at a flow rate of 0.6 ml/min. Fractions (150 μl) were isolated by a Bio-Rad fraction collector. An aliquot of each fraction was used for radioactivity determination and the rest was lyophilized.

Mass Spectrometry. All mass spectra were obtained with a MALDI Bruker Biflex linear time-of-flight mass spectrometer equipped with a scout source and video system, a nitrogen UV laser, and a dual channel plate detector (Bruker Daltonik, Bremen, Germany). The lyophilized fractions were redissolved in 10 μl 90% isopropanol in 0.1% TFA, and a 1-μl aliquot was placed on the MALDI target. One microliter of a freshly prepared saturated solution of α-cyano-4-hydroxycinnamic acid in isopropanol/water/formic acid (2:3:1) was added to this droplet and allowed to dry at room temperature. Spectra were recorded at an acceleration voltage of 35 kV, using initial 2-kV deflection pulses of 2.5 to 3.75 μs perpendicular to the ion flight path for removal of matrix ions. Twenty single laser shots were accumulated into each resulting spectrum. Mass calibration was performed with the singly- and doubly-protonated ions of horse heart cytochrome C.

Results and Discussion

Solubilization of P-gp. The initial step in the analysis of the dexniguldipine binding site was to solubilize, isolate, and purify the [^{3}H]B9209-005–labeled P-gp from the cell membrane preparation of P-gp overexpressing CCRF-ADR5000 cells. Several detergents were examined for their efficiency of P-gp solubilization (Table 1). The solubilization was performed at a detergent concentration of 1% that is above the critical micelle concentration, and nonsolubilized membranes were separated by ultracentrifugation. To quantify the solubilization efficiency, P-gp was prelabeled with [^{3}H]azidopine. The solubilized membranes were analyzed by SDS-PAGE and solubilized P-gp was determined by radioactivity quantification of the excised P-gp band. The solubilities are listed in Table 1 relative to the solubilization obtained with PAGE-sample buffer containing 2% SDS. The nonionic detergents n-octylglucoside and Triton X-100 showed only moderate solubilization efficiency, respectively, whereas the nonionic detergent Nonidet P-40 provided almost complete solubilization. Solubilization efficiencies for the zwitterionic detergents (deoxy-BIGCHAP, CHAPS, Zwittergent 3-12) were also moderate. However, the ionic detergents deoxycholate and N-lauroylsarcosine showed complete solubiliza-

tion, respectively. Considering both the detergent exchange and the detergent removal, as well as compatibility with subsequent purification procedures, *N*-lauroylsarcosine was selected as detergent to solubilize P-gp. Further analysis of *N*-lauroylsarcosine showed that a minimum concentration of 10 to 20 mM was required for a complete solubilization of P-gp (Fig. 1). Therefore, the solubilization was performed in 20 mM *N*-lauroylsarcosine for all subsequent steps.

Purification of [³H]B9209-005–Labeled P-gp. For the purification of solubilized [³H]B9209-005–labeled P-gp, lectin affinity chromatography using RCA-120 was used. The Coomassie-stained gel after separation of the proteins from the eluate (lane 4) and the flow through (lane 3) of the RCA-120 chromatography is shown in Fig. 2a. These analyses were compared with those of the membrane proteins solubilized with either SDS-PAGE sample buffer (lane 1) or *N*-lauroyl-sarcosine (lane 2). The composition and intensity of the proteins in these two samples were identical, demonstrating complete solubilization with *N*-lauroylsarcosine. The protein composition of the flow-through (lane 3) seemed identical with that of the solubilized membranes (lane 2). The intensity of the protein bands from the flow-through, however, was lower because of the dilution from the chromatography. Gel electrophoresis of the eluate (lane 4) showed only a broad band at a molecular mass range of P-gp of 170 to 200 kDa where P-gp is expected. The radioactivity determination of the SDS-gel pieces indicated that the protein band at 170 kDa is [³H]B9209-005–labeled P-gp (Fig. 2b). This analysis also showed the presence of a second [³H]B9209-005–labeled protein at approximately 95 kDa.

For identification of the proteins, Western Blot analysis was carried out using monoclonal anti–P-gp antibody C219 (Fig. 2c) and polyclonal antibody 909 (Fig. 2d) raised against the synthetic peptide, P-gp(909–927). The P-gp protein band was detected by both antibodies in the solubilized membranes (lane 2, 3), in the flow-through (lane 3), and in the elution (lane 4). In addition, the monoclonal antibody C219 that showed antigenic affinity against the N- and C-terminal halves of P-gp (Kartner et al., 1985), detected the 95-kDa band as a P-gp–related protein. The 95-kDa protein was not detected by the polyclonal antibody 909 and was, therefore, assigned as an N-terminal proteolytic P-gp fragment (F1). However, F1 was found in the eluate by silver staining of the

gel (data not shown). Another protein band at 55 kDa was detected in all samples except the elution fraction by both the monoclonal antibody C219 and the polyclonal antibody 909. Therefore, this protein was assigned as the corresponding C-terminal P-gp fragment. In order to obtain larger amounts of purified [³H]B9209-005–labeled P-gp and F1 from solubilized membrane preparations, RCA-120 chromatography was employed in a continuous flow system. The capacity and stability of the RCA-column was assessed by quantification of [³H]B9209-005–labeled P-gp in the different chromatographic steps (Fig. 2e). The radioactivity chromatogram of P-gp showed that the capacity limit of the RCA-120 chromatography was reached at 5 mg of solubilized membrane proteins applied to a 2-ml matrix volume. This corresponds to approximately 30 μg of P-gp based on the ratio of P-gp to total membrane protein estimated to about 0.6% by densitometric determination of the P-gp band after immunoprecipitation (Borchers et al., 1996). Recoveries of P-gp and F1 in the eluate were 32 and 48%, respectively, and decreased by a factor of 2 after each use of the column because of the low stability of the lectins. This is shown by detection of a 30-kDa lectin subunit after gel electrophoresis (Fig. 2a, front of lane 4). In a control experiment it was shown that the instability is at least partially caused by the presence of the detergent *N*-lauroylsarcosine (data not shown).

Trypsin Digestion of Purified, [³H]B9209-005–Labeled P-gp. The [³H]B9209-005–labeled, purified P-gp was digested with trypsin at different concentrations, and the digestion mixture analyzed by SDS-PAGE followed by liquid scintillation counting of the gel slices. In the presence of *N*-lauroylsarcosine, P-gp and F1 were completely resistant to trypsin digestion up to an enzyme to substrate (E/S) ratio of 1:10 (data not shown). For complete digestion of P-gp an E/S of 2:1 was required as shown in Fig. 3, three radioactive, labeled proteolytic fragments with molecular masses of approximately 80, 25, and 8 15 kDa were obtained. At a 10-fold higher enzyme concentration, the fragments of higher molec-

TABLE 1

Efficiency of detergents to solubilize P-gp from plasma membranes of CCRF-ADR5000 cells

Membrane proteins were labeled with 1.6 μM [³H]azidopine, homogenized in the presence of 1% detergent and incubated for 30 min at 4°C. The nonsolubilized membrane proteins were separated by ultracentrifugation, and the supernatant was analyzed by SDS-PAGE. The solubilization efficiency was determined by liquid scintillation counting of the excised radioactive P-gp band. Solubilization of efficiency is given relative to its solubilization with PAGE-sample buffer containing 2% SDS.

Detergent	Solubilization Efficiency [a]
	%
n-Octylglucoside	12
Triton X-100	33
Nonidet P-40	92
Deoxy-BIGCHAP	6
Deoxycholate	47
N-Lauroylsarcosine	103
Zwittergent 3-12	17
CHAPS	3

[a] Standard deviation of the P-gp solubilization efficiency was approximately 5%.
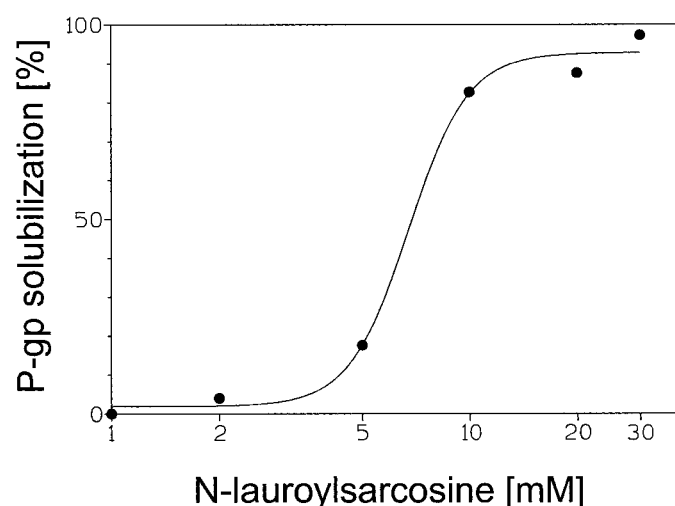

Fig. 1. Solubilization of P-gp in relation to the concentration of the detergent *N*-lauroylsarcosine. In order to quantify the solubilization efficiency, the CCRF-ADR5000 membranes were photolabeled with 0.6 μM azidopine and the solubilized membrane proteins were separated by SDS-PAGE. The amount of solubilized P-gp was determined by radioactivity quantification of the excised P-gp band using liquid scintillation counting. The solubilization of P-gp is shown relative to the solubilization with PAGE-sample buffer containing 2% SDS.
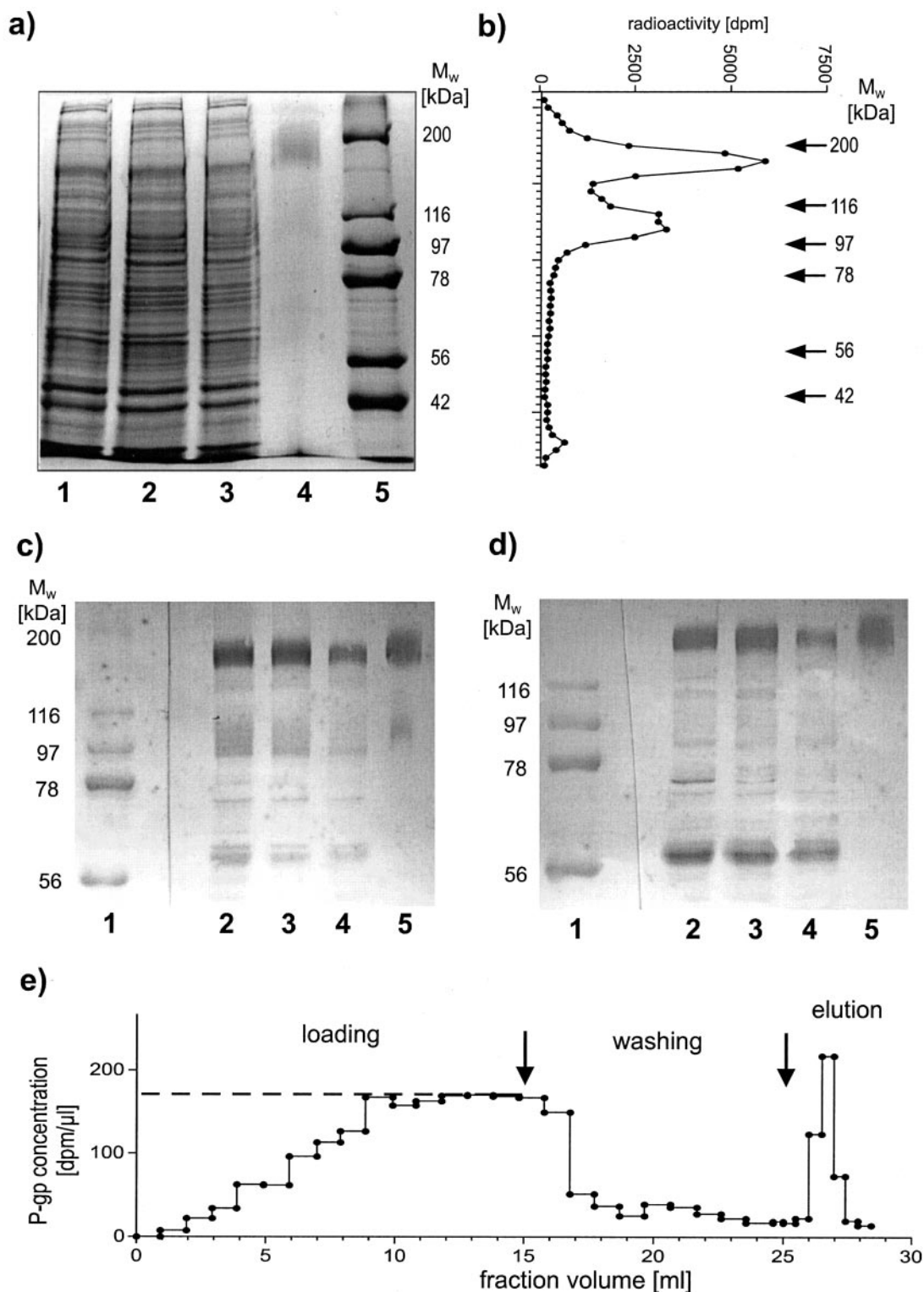
Fig. 2. Purification of P-gp from CCRF-ADR5000 membranes by RCA$_{120}$ lectin-chromatography. RCA-120 column (1.5 ml gel volume) was loaded with 3 ml solubilized (20 mM *N*-lauroylsarcosine) CCRF-ADR5000 membrane proteins after photoaffinity labeling with 1.4 μM [^{3}H]B9209-005 and incubated for 2 h at 4°C. After washing with solubilization buffer the glycoproteins were eluted with 0.2 M methyl-β,D-galactopyranoside. a, Coomassie-staining of the SDS-gel: lane 1, 30 μg of membrane proteins solubilized with SDS-PAGE sample buffer; 2, 30 μg of membrane proteins solubilized with 60 μl of 20 mM *N*-lauroylsarcosine; 3, 60-μl column flow-through; 4, 200-μl elution; 5, molecular mass markers. b, radioactivity determination of SDS-PAGE–separated proteins in the elution. c, Western blot with monoclonal antibody C219. d, Western blot with polyclonal antibody 909. The SDS-gels were loaded with: 1, molecular mass markers; 2, 30-μg membrane proteins solubilized with SDS-sample buffer; 3, 30-μg membrane proteins solubilized with 60 μl of 20 mM *N*-lauroylsarcosine; 4, 60-μl column flow-through; and 5, 114-μl elution. The molecular mass markers on the PVDF-membrane were stained with Ponceau S. RCA-120 chromatography of 2-ml gel volume by in continuous flow (1 ml/min). 1, loading: 15 ml of solubilized (20 mM *N*-lauroylsarcosine) plasma membranes (7.5 mg) after photoaffinity labeling with 1.2 μM [^{3}H]B9209-005; 2, washing: 10 ml of solubilization buffer (20 mM *N*-lauroylsarcosine); 3, elution: 0.2 M methyl-β,D-galactopyranoside in solubilization buffer. P-gp concentration in the fractions (0.5–1 ml) was determined by radioactivity determination of the excised P-gp band in the SDS-gel from the PAGE of the individual fractions.

ular mass were further digested concomitant with a decrease of the 8- to 15-kDa fragment containing 57% of the initial radioactivity of P-gp and F1. Furthermore, high E/S (20:1) led to increased tryptic auto-proteolytic peptides, which might interfere with the mass spectrometric analysis. Increasing the reaction time of the proteolysis while using less enzyme was also unsuccessful because of a progressive decrease of the P-gp recovery with time.

In contrast to the proteolysis in *N*-lauroylsarcosine, lower E/S ratios were sufficient to produce low-molecular-mass tryptic fragments using the detergents CHAPS (E/S = 10:1) and *n*-octylglucoside (E/S = 1:5). Furthermore, the detergent exchange of *N*-lauroylsarcosine against CHAPS and *n*-octyl-glucoside (performed by ultra-filtration) provided complete separation of the lectin subunit from P-gp and F1. The radiogram of the SDS-PAGE analysis of the peptide mixture

obtained by digestion in *n*-octylglucoside showed a single peak corresponding to a [^{3}H]B9209-005-bound polypeptide of 7 to 8 kDa (Fig. 4a) with a shoulder at ~5 kDa indicating an additional [^{3}H]B9209-005-bound peptide. The proteolysis in CHAPS led to the formation of two [^{3}H]B9209-005–bound peptides with molecular masses of approximately 15 and 8 kDa (Fig. 4b). However, because aggregation occurred in the presence of CHAPS as shown by a front peak in the stacking gel (Fig. 4b), the tryptic digestion in the following experiments was performed in *n*-octylglucoside.

HPLC Isolation of the [^{3}H]B9209-005–bound Peptides. Because of the complexity of the mixture of tryptic peptides from P-gp (179 possible cleavage sites) and contamination with auto-proteolytic tryptic peptides isolation of [^{3}H]B9209-005–bound peptides was necessary before mass spectrometric analysis. For the isolation of the [^{3}H]B9209-
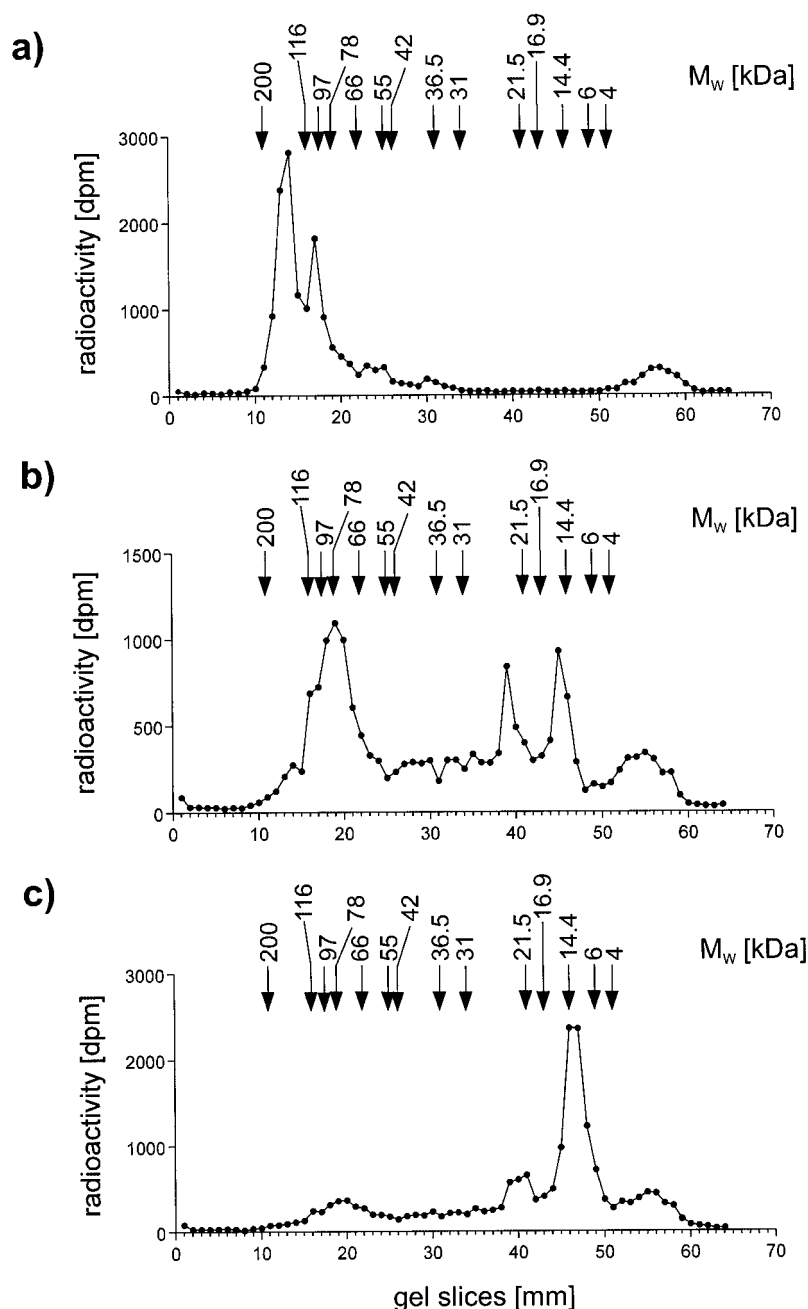

Fig. 3. Gel electrophoretic analysis of the tryptic digestion of [^{3}H]B9209-005–labeled, affinity-purified P-gp/F1 in *N*-lauroylsarcosine. Digestion was carried out for 2.5 h at 37°C with different amounts of trypsin. The separation of the proteolytic digestion mixture was performed by a 7.5 to 20% polyacrylamide gradient gel. a, RCA-120 chromatography; b, proteolysis with 10 μg trypsin/ml; c, proteolysis with 100 μg trypsin/ml.

005–bound peptides, reversed-phase HPLC (C4) was performed with an isopropanol/acetonitrile mixture as the organic mobile phase. Control experiments showed that the photoinduced linkage between [³H]B9209-005 and P-gp was sufficiently stable under these HPLC conditions. Figure 5 shows the HPLC UV chromatogram of the tryptic digest of [³H]B9209-005–labeled P-gp and its radiogram, as well as the UV chromatogram of trypsin after autoproteolysis. The radiogram showed two signals, with a peak at longer retention time (Fig. 5a, signal 2) containing two [³H]B9209-005–bound peptides with molecular masses of 8 to 10 and 5 kDa as shown by SDS-PAGE analysis (data not shown). The SDS-PAGE analysis of signal 1 showed free [³H]B9209-005, indicating some instability of the [³H]B9209-005–bound peptides in signal 2 (data not shown). It is known that photoinduced ligand-peptide bonds of certain azido-photoaffinity ligands can dissociate under HPLC conditions (Salvucci et al., 1992). However, no peak at the retention time of signal 2 was detected in the UV chromatogram of the trypsin auto-proteolysis products (Fig. 5c), indicating that this fraction did not contain autoproteolytic fragments.

Mass Spectrometric Characterization of the [³H]B9209-005–bound Peptides. To identify the tryptic [³H]B9209-005–bound peptides, the HPLC fractions corresponding to signal 2 were pooled and analyzed by MALDI mass spectrometry (MS). The MALDI-mass spectra revealed three intense ion signals at m/z 5230, 5734, and 7416 (Fig. 6). The same ions were obtained after incubation with 2-mercaptoethanol, indicating that these peptides do not correspond to disulfide-linked sequences (data not shown). For assignment, the masses of these ions were compared with the masses of the tryptic peptides calculated from the amino acid sequence with and without the incorporation of one dexnigul-

dipine molecule providing a mass increment of 577 amu based on simple carbon bond insertion of the photoaffinity binding. At the MALDI mass determination accuracy (~0.1%), no single mass assignment was obtained (Table 2); however, the fragment at m/z 7416 provided a single candidate sequence containing a dexniguldipine moiety.

The combined Edman-MS sequencing method after coupling with phenylisothiocyanate was applied for further identification (Nielsen et al., 1990). In contrast to conventional Edman sequencing, the combined Edman-MS method analyses the peptides remaining after successive cleavage of the N-terminal amino acids by mass spectrometry. Furthermore, useful information can be gained by mass spectrometric analysis of the PTC-adducts after the Edman coupling step which can reveal the maximum number of free amino groups (ϵ-amino groups of lysine residues) and free thiol groups (cysteine residues) in the peptide. MALDI-MS analysis of the PTC-adducts of the fractions corresponding to the HPLC-signal 2 showed ion signals at m/z 8137, m/z 6624 and m/z 5514 (Table 3). A control MALDI experiment of the reaction mixture in the absence of PITC showed no differences before and after the Edman coupling step (data not shown), indicating that the [³H]B9209-005-bound peptide was stable under these conditions.

Assignment of [³H]B9209-005–Bound Peptides. Assigning a mass increment of 577 amu per dexniguldipine and of 135 amu per PTC molecule, the molecular mass increase for the three ions at m/z 7416, m/z 5734, and m/z 5230 corresponds to incorporation of 5, 3, and 2 PTC-molecules, respectively. This means that the ion at m/z 7416 can only be assigned to a peptide containing at least four lysine residues, hence it can only be assigned to the [³H]B9209-005–bound P-gp peptide sequence, 468–527 (Table 3). The ion at m/z
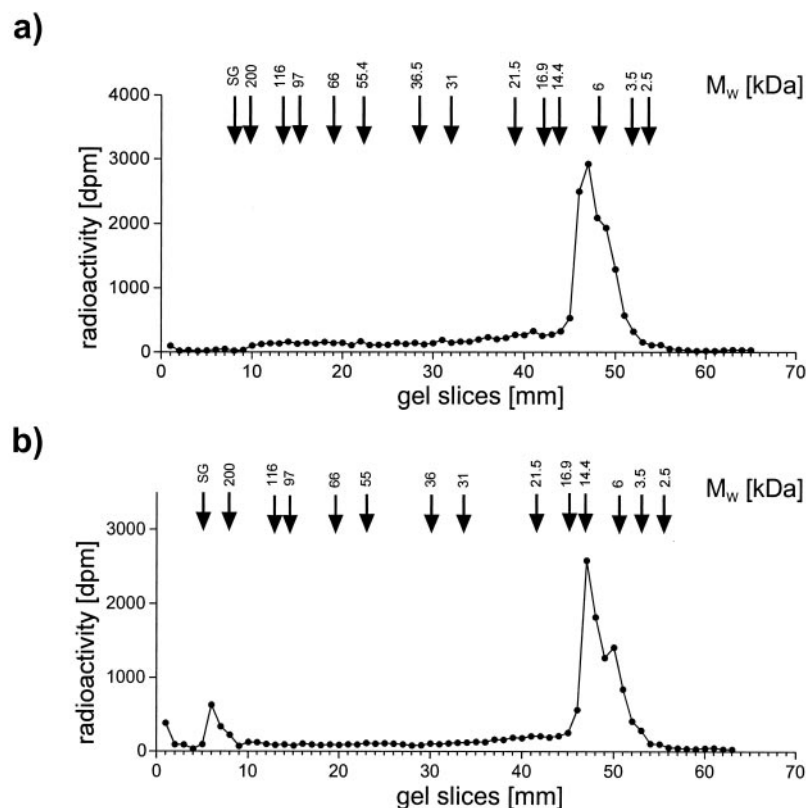
a)

b)

Fig. 4. Gel electrophoresis of the tryptic digestion of [³H]B9209-005–labeled, affinity-purified P-gp/F1 in the presence of 1.4% n-octylglucoside (a) and 1% CHAPS (b). The detergent exchange (N-lauroylsarcosine against n-octylglucoside or CHAPS) was carried out by ultra-filtration after the RCA-120 chromatography. Proteolysis was performed for 2.5 h at 37°C with an E/S of 10:1. For separation of the proteolytic digest, a 7.5 to 20% polyacrylamide SDS-gradient gel was used.

5734 was assigned to the tryptic P-gp peptide 620–670 because this peptide contains three lysine residues. The mass spectrometric analysis of the Edman coupling product of the ion at *m/z* 5230 could not be unambiguously assigned because the two possible peptides possess more than one lysine resi-

Fig. 5. HPLC analysis of the tryptic digestion of [³H]B9209-005–labeled, affinity-purified P-gp/F1. Proteolysis was performed with 100 μl/mg trypsin in 1.4% *n*-octylglucoside for 2.5 h at 37°C. An aliquot of 72 μl of the proteolytic digestion was applied on a C4-column and a 10 to 90% gradient of 0.1% in isopropanol/acetonitrile (4:1, v/v) was used. a, radioactivity of the HPLC-fractions (150 μl) was determined by scintillation counting of an aliquot of an 25 μl aliquot; b, UV-absorption (220 nm); c, UV-absorption (220 nm) of control tryptic autoproteolytic mixture.

Fig. 6. MALDI mass spectrometric analysis of the HPLC fraction (42 min, signal 2 in Fig. 5) from the tryptic digestion of [³H]B9209-005–labeled, affinity-purified P-gp/F1. The mass spectrum was calibrated with cytochrome *c*.

due (Table 3). Nevertheless, this result does not preclude the assignments in Table 3, because the number of incorporated PITC groups is not necessarily the sum of N-terminal amino groups and all lysine residues. Thus, incomplete coupling of the amino groups with PITC has been shown for hen egg lysozyme and the disulfonated insulin B-chain (Nielsen et al., 1990). The MALDI mass spectra of samples obtained after Edman cleavage of PTC coupling products did not yield interpretable results because of low ion abundance and signal-to-noise ratios, and possible decomposition of dexniguldipine adducts.

Conclusions

In this study, we have identified the interacting binding site of the chemosensitizer dexniguldipine, a dihydropyridine derivative, in human P-gp using a combination of photoaffinity and mass spectrometric approaches. For photoaffinity labeling, the tritiated dexniguldipine analog [³H]B9209-005 was used, which has chemosensitizing potency identical to that of dexniguldipine and is, therefore, suitable for elucidation of the binding sites (Boer et al., 1996; Borchers et al., 1996). The mass spectrometric analysis localized the dexniguldipine binding site to the P-gp sequence 468–527, in agreement with previous immunoprecipitation experiments showing that the dexniguldipine binding site is in the N-terminal half of the protein P-gp (Borchers et al., 1996). This sequence region is flanked by the Walker motifs A and B of the N-terminal ATP-binding cassette.

The model of human P-gp based on hydropathy analysis (Gottesman and Pastan, 1988) suggests that the sequence region 468–527 is localized in the cytoplasm which is in agreement with previous binding analysis of dexniguldipine to membranes of CCRF-ADR5000 cells (Ferry et al., 1992). In addition, recent photoaffinity labeling competition studies with [³H]B9209-005 in whole cells and [³H]vinblastine binding analysis have shown that dexniguldipine blocks vinblastine binding, and thereby transport by P-gp, by acting at a domain accessible only from the cytoplasm (Ferry et al., 2000). However, the binding sequence identified is significantly different from the previously postulated major binding sites of chemomodulators and cytostatics in the transmembrane domains 5, 6 and 11, 12 and their connecting extracellular loops. These data were based mainly on immunological analysis of P-gp proteolytic fragments after photoaffinity labeling with [³H]azidopin (Bruggemann et al., 1989; 1992; Yoshimura et al., 1989), ¹²⁵I-forskolin derivatives (Morris et al., 1994), and ¹²⁵I-arylazidoprazosin (Greenberger et al., 1991). However, mutation studies have supported these results, suggesting that other regions may also play an important role in defining the drug-binding domain (Ambudkar et al., 1999). In more recent studies, further analytical approaches have been used to identify the photo-affinity labeled binding sites of cytostatics and chemosensitizers. Using Edman sequencing of radiolabeled peptides, the binding site of iodomycin (the Bolton-Hunter derivative of the anthracycline daunomycin) was localized to amino acids (aa) 230 to 312 of hamster P-gp. This region, according to the hydrophobicity model of Gottessmann and Pastan (1988), forms the distal part of TM4 (the second cytoplasmic look) and the proximal part of TM5 (Demmer et al., 1997). Applying the same analytical approach, three binding sites of iodoarylazidoprazosin
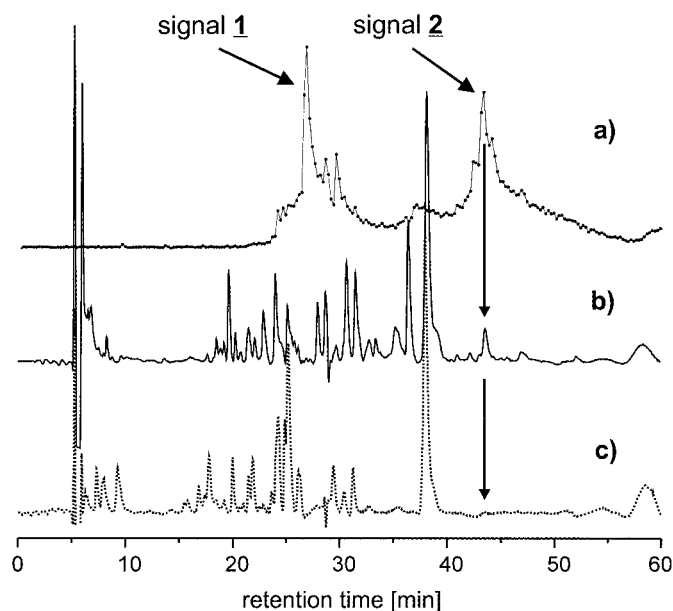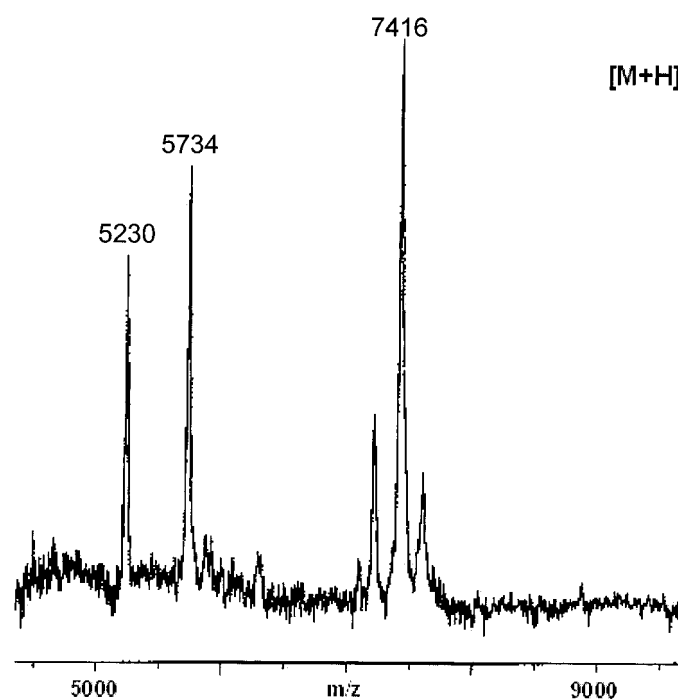
TABLE 2

Assignment of ion signals determined by MALDI-MS analysis of the radioactive HPLC-fraction (signal 2 in Fig. 6) from the tryptic digestion of [³H]B9209-005–labeled P-gp/F1.

Photochemical incorporation of dexniguldipine leads to a mass increment of 577 amu. Molecular mass was calculated from the amino acid sequence.

MALDI-MS	Dexniguldipine Incorporation[a]	Tryptic P-gp Peptide	Lysine Residues	Molecular Mass (Theoretical)
m/z		*aa*		*Da*
7416	−	147–210	3	7417
	+	443–502	1	7420
	+	468–527	4	7418
5734	−	620–670	3	5735
	+	1015–1061	1	5734
5230	−	620–666	3	5235
	+	618–659	3	5228

+, incorporation of dexniguldipine; −, no incorporation.

TABLE 3.

MALDI-MS data of P-gp peptides (HPLC signal 2) after one Edman coupling step with phenylisothiocyanate

MALDI mass spectrometric analysis of the [³H]B9209-005– bound P-gp peptide (fraction of HPLC signal 2 in Fig. 6) after first Edman coupling procedure. For the Edman coupling, the lyophilized HPLC fraction was incubated with 5% PITC for 4 h at 30°C. The ion signals in the spectrum are labeled with the average mass and the number of phenylthiocarbamoyl (PTC) groups that are incorporated (compare Fig. 7).

MALDI-MS	PTC Residues Incorporated[a]	Sequence	Unmodified Peptide Molecular Mass[b]	Dexniguldipine Incorporation[b]	Number of Lysine Residues
m/z		*aa*	*Da*		
8137	5	468–527	7418	+	4
6224	3–4	620–670	5735	−	3
5514	2	620–666	5228	−	3
		618–659		+	3

[a] Mass increment of PTC, 135 amu.
[b] Compare Table 2.

were found in the regions of aa 248 to 312 (TM4 to TM5), aa 758 to 800 (beyond TM8), and aa 1160 to 1218, which are located within the second cytosolic NBD (Isenberg et al., 2001). Using overlapping peptide mapping with different chemical cleavage agents and immunoprecipitation, the binding site of cyclosporin A was localized to aa 953 to 1007, a region between the end of TM11 and the end of TM12 (Demeule et al., 1998). It is worth noting that cyclosporin A as well as viblastine bind with high affinity to the iodomycin binding site (see above) (Demmer et al., 1997). Using benzophenone analogs the binding domain of paclitaxel has been localized to aa 683 to 760 (including TM7 and TM8) and 985 to 1088, a region that includes half of TM12 and terminates just after the Walker A motif in the second nucleotide binding site (Wu et al., 1998). It is important that the labeling of the binding site depends on the position of the benzophenone group in paclitaxel. All these results suggest that the drug/chemosensitizer binding sites of P-gp form a complex three-dimensional structure within the transmembrane and cytosolic domains, including the NBDs. Cross-linking

experiments of the TMs 4 to 6 and 10 to 12 suggest that the drug binding domain is funnel-shaped, narrow at the cytoplasmic side (9–25 Å), and wider at the extracellular surface (Loo and Clarke, 2001). The different drug binding sites in our results may be explained by the different position of the photoactivatable group (azido group) in other ligands compared with [³H]B9209-005. In all these photoaffinity ligands, the azido group is located in the hydrophobic site chain, whereas the azido group in [³H]B9209-005 is directly in the pharmocophore, dihydropyridine moiety.

In a recently proposed structural model of P-gp (Jones and George, 1998), the dexniguldipine binding site corresponds to a region composed of two membrane-spanning β-strands (β-15 and β-16) followed by a cytosolic loop-helix (α-6) component (Fig. 7). If the dexniguldipine binding site is in a cytoplasm-localized P-gp region (Ferry et al., 1992), the binding site in this model can be assigned to the sequence 491–526, which includes the loop-(α-6)-helix component. The model suggests that this region is near the Walker A and B motifs of the N-terminal nucleotide binding site, indicating
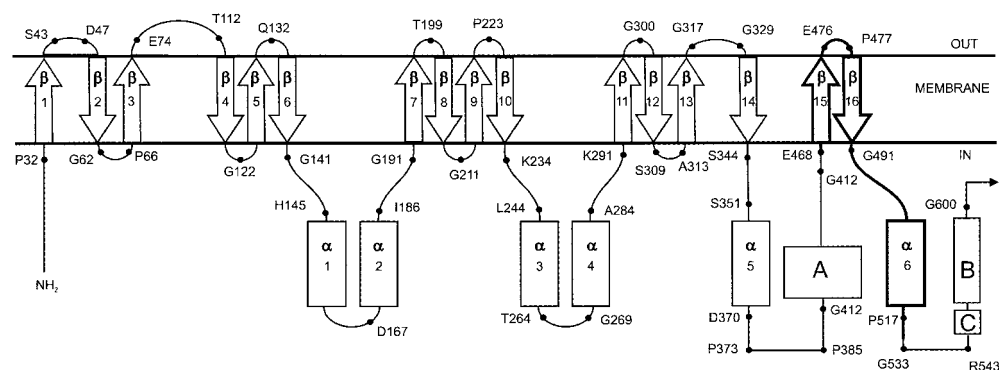

Fig. 7. Dexniguldipine-HCl binding sequence in the topological P-gp model according to Jones and George (1998). The N-terminal is suggested to consist of 16 transmembrane β-sheets (arrowed rectangles) and six cytoplasmic α-helices (rectangles). The lettered boxes A (Walker A motif), C (dodecapeptide), and B (Walker B motif) represent the ATP domains. The numbered residues are co-ordinate signposts for the topology. The dexniguldipine-HCl binding sequence 468–527 is highlighted in bold.

that the chemosensitizer binding site and ATP binding/utilization domains interact directly with each other.

It is well known that drug binding and ATP hydrolysis sites, as well as the chemosensitizer site and the ATP hydrolysis, are intimately coupled (Ramachandra et al., 1998). Kinetic studies using [³H]vinblastine binding competition analysis also elucidated that the binding of nucleotides to P-gp reduces availability of the drug binding sites (Martin et al., 2000). However, the mechanism of these interactions is not clearly understood. More detailed structure-function analyses at the molecular level are necessary to elucidate a three-dimensional structure of the interaction site, which should provide a better understanding of the mechanism of action of P-gp. A recent structural study using cryomicroscopy of two-dimensional crystals yielded an 10-Å resolution structure of P-gp, which has shown that nucleotide binding causes a repacking of the transmembrane domains and a reduction of the drug binding affinity, thus confirming and explaining the results of kinetic studies (Rosenberg et al., 2001). As shown in this study, the combination of photoaffinity labeling and mass spectrometry is an efficient molecular approach to identify the binding sequences. Furthermore, most recent MS developments, such as tandem-MS and high-resolution Fourier transform MS techniques, have the potential to identify ligand-interacting amino acids precisely (Borchers et al., 1999; Fligge et al., 2000; Bauer et al., 2001; Kohlmann et al., 2002; Przybylski et al., 2002). Furthermore, photoaffinity labeling experiments using ligands with the photoactivable group at different positions allow the identification of the ligand-interacting amino acids in the binding area. Such data should provide constraints that can be used in computational chemistry to model the three-dimensional structure of the binding site which is essential for understanding the mechanism of P-gp and for the structure-based design of chemosensitizers.

Acknowledgments

References

Ambudkar SV, Dey S, Hrycyna CA, Ramachandra M, Pastan I, and Gottesman MM (1999) Biochemical, cellular, and pharmacological aspects of the multi-drug transporter. *Annu Rev Pharmacol Toxicol* **39:**361–391.

Azzaria M, Schurr E, and Gros P (1989) Discrete mutations introduced in the predicted nucleotide-binding sites of the *mdr1* gene abolish its ability to confer multi-drug resistance. *Mol Cell Biol* **9:**5289–5297.

Bauer SH, Wiechers MF, Bruns K, Przybylski M, and Stuermer CAO (2001) Isolation and identification of the plasma membrane-associated intracellular protein reggie-2 from goldfish brain by chromatography and Fourier transform-ICR mass spectrometry. *Anal Biochem* **298:**25–31.

Boer R, Ulrich W-R, Haas S, Borchers C, Gekeler V, Boss H, Przybylski M, and Schödl A (1996) Interaction of cytostatics and chemosensitizers with the dexniguldipine binding site on P-glycoprotein. *Eur J Pharmacol* **295:**253–260.

Borchers C, Boer R, Conrad J, Gekeler V, Ulrich WR, Ise W, Klemm K, and Przybylski M (1996) Photoaffinity labeling with a photoreactive analogue of dexniguldipine HVCl (B850S-035) and mass spectrometric stuctural characterzation of the multidrug resistance-related P-glycoprotein, in *Peptides 1994* (Maia H ed), pp 803, Escom, Leiden.

Borchers C, Parker CE, Deterding LJ, and Tomer KB (1999) Preliminary comparison of precursor scans and liquid chromatography-tandem mass spectrometry on a hybrid quadrupole time-of-flight mass spectrometer. *J Chromatogr A* **854:**119–130.

Borchers C, Ulrich W-R, Klemm K, Ise W, Gekeler V, Haas S, Schödl A, Conrad M, Przybylski M, and Boer R (1995) B9209-005, an azido-derivative of the chemosensitizer dexniguldipine-HCl photolabels P-glycoprotein. *Mol Pharmacol* **48:**21–29.

Bruggemann EP, Currier SJ, Gottesman MM, and Pastan I (1992) Characterization of the azidopine and vinblastine binding site of P-glycoprotein. *J Biol Chem* **267:**21020–21026.

Bruggemann EP, Germann UA, Gottesman MM, and Pastan I (1989) Two different

regions of P-glycoprotein are photoaffinity-labeled by azidopine. *J Biol Chem* **264:**15483–15488.

Chen C-J, Chin JE, Ueda K, Clark DP, Pastan I, Gottesman MM, and Roninson IB (1986) Internal duplication and homology with bacterial transport proteins in the mdr1 (P-glycoprotein) gene from multi-drug-resistant human cells. *Cell* **47:**381–389.

Demeule M, Ladplante A, Murphy GF, Wenger RM, and Beliveau R (1998) Identification of the cyclosporin-binding site in P-glycoprotein. *Biochemistry* **27:**18110–18118.

Demmer A, Thole H, Kubesch P, Brandt T, Raida M, Fislage R, and Tuemmler B (1997) Localization of the iodomycin binding site in hamster P-glycoprotein. *J Biol Chem* **272:**20913–20919.

Endicott JA and Ling V (1989) The biochemistry of P-glycoprotein-mediated multidrug resistance. *Annu Rev Biochem* **58:**137–171.

Ferry D, Boer R, Callaghan R, and Ulrich WR (2000) Localization of the 1,4-dihydropyridine drug acceptor of P-glycoprotein to a cytoplasmic domain using a permanently charged derivative *N*-methyl dexniguldipine. *Int J Clin Pharmacol Ther* **38:**130–140.

Ferry DR, Russel MA, and Cullen MH (1992) P-glycoprotein possesses a 1,4 dihydropyridine-selective drug acceptor site which is allosterically coupled to a Vinca alkaloid-selective binding site. *Biochem Biophys Res Commun* **188:**440–445.

Fisher GA, Halsey J, Hausdorff J, Lum N, Brophy NA, Collins N, Nix D, and Sikic BI (1994) A phase I study of paclitaxel (Taxol) (T) in combination with SDZ PSC 833, a potent modulator of multi-drug resistance (MDR). *Anti-Cancer Drugs* **5(Suppl 1):**43.

Fligge TA, Reinhard C, Harter C, Wieland FT, and Przybylski M (2000) Oligomerisation of peptides analogous to the cytoplasmic domains of coatamer receptors revealed by mass spectrometry. *Biochemistry* **39:**8491–8496.

Gottesman MM and Pastan I (1993) Biochemistry of multidrug resistance mediated by the multidrug transporter. *Annu Rev Biochem* **62:**385–427.

Gottesman MM and Pastan I (1988) The multi-drug-transporter: a double-edged sword. *J Biol Chem* **263:**12163–12166.

Greenberger LM (1998) Identification of drug interaction sites in P-glycoprotein. *Methods Enzymol* **292:**307–317.

Greenberger LM, Lisanti CJ, Silva JT, and Horwitz SB (1991) Domain mapping of the photoaffinity drug-binding sites in P-glycoprotein encoded by mouse mdr1b. *J Biol Chem* **266:**20744–20751.

Hayes JD and Wolf CR (1990) Molecular mechanism of drug resistance. *Biochem J* **272:**281–295.

Hofmann J, Gekeler V, Ise W, Noller A, Mittendorfer J, Hofer S, Utz I, Gotwald M, Boer R, Glossmann H, and Grunicke H (1995) Mechanism of action of dexniguldipine-HCl (B8509-035), a new potent modulator of multidrug resistance. *Biochem Pharmacol* **49:**603–609.

Isenberg B, Thole H, Tuemmler B, and Demmer A (2001) Identification and localization of three photobinding sites of iodoarylazidoprazin in hamster P-glycoprotein. *Eur J Biochem* **268:**2629–2634.

Jones PM and George AM (1998) A new structural model for P-glycoprotein. *J Membr Biol* **15:**133–147.

Juranka PF, Zastawny RL, and Ling V (1989) P-glycoprotein: multidrug-resistance and a superfamily of membrane-associated transport proteins. *FASEB J* **3:**2583–2592.

Kartner N, Everndenporelle D, Bradley G, and Ling V (1985) Detection of P-glycoprotein in multi-drug-resistant cell-lines by monoclonal-antibodies. *Nature (Lond)* **316:**820–823.

Kimming A, Gekeler V, Neumann M, Frese G, Handgretinger R, Kardos G, Diddens H, and Niethammer D (1990) Susceptibility of multidrug resistant human leukemia cell lines to human interleukin 2-activated killer cells. *Cancer Res* **50:**6793–6799.

Kohlmann M, Bruns K, Castagnos A-M, and Przybylski M (2002). Mass spectrometric identification of a C-terminal epitope of amyloid precursor protein (APP). *Anal Bioanal Chem*, in press.

Loo TW and Clarke DM (2001) Determining the dimensions of the drug-binding domain of human P-glycoprotein using thiol cross-linking compounds as molecular rulers. *J Biol Chem* **276:**36877–36880.

Martin C, Berridge G, Mistry P, Charlton P, Higgins CF, and Callaghan R (2000) Drug binding sites are altered by ATP binding prior to nucleotide hydrolysis. *Biochemistry* **39:**11901–11906.

Morris DI, Greenberger LM, Bruggemann EP, Cardarelli C, Gottesman MM, Pastan I, and Seamon KB (1994) Localization of the forskolin labeling sites to both halves of P-glycoprotein: similarity of the sites labeled by forskolin and prazosin. *Mol Pharmacol* **46:**329–337.

Nielsen PF, Schneider K, Suckau D, Landis B, and Przybylski M (1990) Applications of selective chemical reactions in combination with 252-californium plasma desorption mass spectrometry in protein structure analysis, in *Mass Spectrometry of Large Non-Volatile Molecules* (Hilf E ed), pp 194–207, World Scientific, London.

Presant CA, Kennedy P, Wiseman C, Galla K, and Wyres M (1984) Verapamil plus adriamycin: a phase I-II clinical study. *Proc Am Soc Clin Oncol* **3:**32.

Przybylski M, Schnaible V, Kast J, Bühler S, Michels J, Wattenberg A, Fligge TA, Forst D, Diederichs K, Zeth C, et al. (1998) Approaches to the characterization of tertiary and supramolecular protein structures by combination of protein chemistry and mass spectrometry, in *New Methods for the Study of Biomolecular Complexes*, pp 17–43, Kluwer Academic Publishers, Amsterdam.

Przybylski M, Youhnovski N, Bruns K, Damoc E, Rossier J, Reymond F, Damoc C, Knippers R, Cecal R, and Tian X (2002) Approaches and applications of Fourier transform ion cyclotron resonance mass spectrometry to proteome analysis with high resolution and high selectivity. *Proteomics*, in press.

Raderer M and Scheithauer W (1993) Clinical trials of agents that reverse multidrug resistance. *Cancer (Phila)* **72:**3553–3563.

Ramachandra M, Ambudkar SV, Chen D, Hrycyna CA, Dey S, Gottesman MM, and

Pastan I (1998) Human P-glycoprotein exhibits reduced affinity for substrates during a catalytic transition state. *Biochemistry* **37:**5010–5019.

Reiter WW, Ludescher C, Wörmann B, Nüßler V, Gattringer C, Reiber C, Weimar C, Nowrousian MR, and Thaler J (1994) A phase II trial with dexniguldipine, a new multidrug resistance modulator in combination with VAD or VECD iin patients with refractory myeloma (Abstract). *Ann Oncol* **5(Suppl):**136.

Rosenberg MF, Callaghan R, Ford RC, and Higgins CF (1997) Structure of the multidrug resistance P-glycoprotein to 2.5 nm resolution determined by electron microscopy and image analysis. *J Biol Chem* **272:**10685–10694.

Rosenberg MF, Velarde G, Ford RC, Martin C, Berridge G, Kerr ID, Callaghan R, Schmidlin A, Wooding C, Linton KJ, et al. (2001) Repacking of the transmembrane domains of P-glycoprotein during the transport ATPase cycle. *EMBO (Eur Mol Biol Organ)* **20:**5615–5625.

Safa AR (1998) Photoaffinity labels for characterizing drug interaction sites of P-glycoprotein. *Methods Enzymol* **292:**289–307.

Salvucci ME, Chavan AJ, and Haley BE (1992) Identification of peptides from the adenine binding domains of ATP and AMP in adenylate kinase—isolation of photoaffinity-labelled peptides by metal chelate chromatography. *Biochemistry* **31:**4479–4497.

Sikic BI (1993) Modulation of multidrug resistance: at the threshold. *J Clin Oncol* **11:**1629–1635.

Urbatsch IL, Sankaran B, Bhagat S, and Senior AE (1995) Both P-glycoprotein nucleotide-binding sites are catalytically active. *J Biol Chem* **270:**26956–26961.

Wu Q, Bounaud P-Y, Kuduk SD, Yang C-Ph, Howitz SB, and Orr GA (1998) Identification of the domains of photoincorporation of the 3′- and 7-benzophenone analogues of Taxol in the carboxy-terminal half of murine mdr1b P-glycoprotein. *Biochemistry* **37:**11272–11279.

Yoshimura A, Kuwazuru Y, Sumizawa T, Ichikawa M, Ikeda S, Uda T, and Akiyama S (1989) Cytoplasmic orientation and two-domain structure of the multidrug transporter, P-glycoprotein, demonstrated with sequence-specific antibodies. *J Biol Chem* **264:**16282–16291.

Address correspondence to: Dr. Michael Przybylski, Department of Chemistry, Laboratory of Analytical Chemistry, University of Konstanz, 78457 Konstanz, Germany. E-mail: michael.przybylski@uni-konstanz.de